NJC

New Journal of Chemistry

A journal for new directions in chemistry

Accepted Manuscript

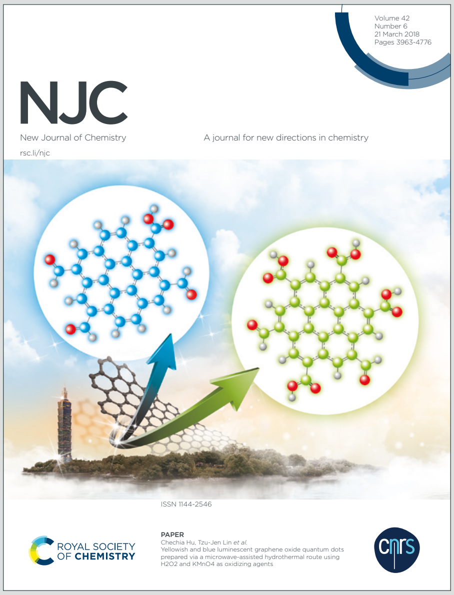

ROYAL SOCIETY OF CHEMISTRY

rsc.li/njc

COMMUNICATION

Hypotoxic synthesis of Co_2P nanodendrite for boosting ammonia electrosynthesis from nitrate

Received 00th January 20xx,
Accepted 00th January 20xx

DOI: 10.1039/x0xx00000x

Luocai Yi[a]*, Ping shao[a], Zhenhai Wen[a]*

High-quality Co_2P nanodendrites are one-step prepared using a molten-salt-assisted synthesis method, which avoids the release of highly toxic phosphine and the use of flammable organic phosphorus sources. Electrochemical measurements reveal that Co_2P nanodendrites can be used as an efficient electrocatalyst for ammonia (NH_3) synthesis from nitrate reduction reaction (NO_3^-RR) in a neutral electrolyte. At an applied potential of -0.6 V vs. reversible hydrogen electrode, Co_2P nanodendrites can operate stably for 10 continuous cycles, and the average faradic efficiency and yield rate of ammonia generation are 88.57% and 5.11 mg cm^{-2} h^{-1}, respectively. Thus, the present results will provide new insights into the synthesis of phosphides and the development of NO_3^-RR catalysts.

Ammonia (NH_3) is one of the extremely important industrial products for food production as it is an essential feedstock for N-based fertilizers and is emerging as a potentially sustainable liquid fuel and as a critical hydrogen carrier.[1, 2] Currently, the traditional Haber-Bosch (H-B) process ($N_2(g)+3H_2(g) \rightleftharpoons 2NH_3(g)$) dominates scalable industrial NH_3 synthesis, requiring huge amounts of energy and, thus, causing pollution.[3, 4] As a result, we need to develop sustainable alternative ways to the H-B process in response to the global energy and environmental crisis. The aqueous-based electrochemical synthesis of NH_3 has been recognized as one of the most attractive approaches for NH_3 production ascribed to utilizing renewable electricity, operating at ambient conditions, and does not require additional hydrogen supply.[5-7] Numerous attempts at aqueous-based electrochemical reduction of nitrogen to NH_3 have been carried out over the years. Unfortunately, due to the inherent inertia of N≡N (bond energy: 941 kJ mol^{-1}), limited nitrogen solubility, and the competitive hydrogen evolution reaction (HER), result in the formation rate, selectivity, and Faraday efficiency of nitrogen electroreduction to NH_3 are far from meeting the application requirements.[8, 9] By contrast, the electrochemical reduction of nitrate to NH_3 (nitrate reduction reaction, NO_3^-RR, $NO_3^- + 6H_2O + 8e^- \rightarrow NH_3 + 9OH^-$) represents an alternative and attractive route for sustainable ambient NH_3 synthesis owing to nitrate high solubility in aqueous solutions and low dissociation energy of N=O (204 kJ mol^{-1}).[10-14] Moreover, nitrate is also a contaminated source unhealthy has been linked to increased risk for various types of cancer in humans.[15, 16] Therefore, the electroreduction of nitrate to ammonia is expected to alleviate multiple crises in energy, environment, and ecology.

Although various heterogeneous noble metals electrocatalytic (such as Au,[17] Ag,[18] Pt,[19] Ru,[20] Rh,[21] Pd,[22] etc.) have been developed for NO_3^-RR, their scarcity and price make them unsuitable for large-scale applications. Consequently, considerable efforts have been spent developing earth-abundant transition metal-based (such as copper-based,[23-25] cobalt-based,[26-31] iron-based,[32, 33] nickel-based,[34-37] *etc.*) electrocatalytic for their utilization in NO_3^-RR. Among them, cobalt-based (such as cobalt metal,[27, 38, 39] phosphide,[40, 41] oxide,[26, 42] *etc.*) catalytic have been proved theoretically and experimentally to be highly selective in the electroreduction of nitrate to ammonia. In particular, cobalt phosphide shows an impressive Faraday efficiency of nearly 100% in the electrocatalysis conversion of nitrite to ammonia.[40] Among Co_2P, the metalloid properties make it highly favored in the field of electrocatalysis due to its exceptional conductivity.[43] However, the existing synthesis process of metal phosphides generally has potential safety hazards, such as releasing highly toxic substances (NaH_2PO_2 pyrolysis to PH_3) or using flammable phosphorus sources, so it is urgent to develop a simple and low-toxic synthesis approach.[44]

Herein, we report a molten-salt-assisted synthesis method without phosphine release and a flammable phosphorus source to synthesize dicobalt phosphide (Co_2P) nanodendrites. The as-

---

[a] *Address here. CAS Key Laboratory of Design and Assembly of Functional Nanostructures, and Fujian Provincial Key Laboratory of Materials and Techniques toward Hydrogen Energy, Fujian Institute of Research on the Structure of Matter, Chinese Academy of Sciences, Fuzhou, Fujian, 350002, China.*

* *Corresponding author, Email: lcyi@fjirsm.ac.cn, wen@fjirsm.ac.cn.*

† Footnotes relating to the title and/or authors should appear here.

Electronic Supplementary Information (ESI) available: [details of any supplementary information available should be included here]. See DOI: 10.1039/x0xx00000x prepared Co_2P nanodendrites were applied as an efficient electrocatalyst toward the NO_3^-RR in the neutral electrolyte, including a high selectivity (88.57%), yield rate (5.11 mg cm^{-2} h^{-1}), and stability (10 cycles) for NH_3 production.

Co_2P nanodendrites were achieved through a one-step procedure ($2Co^{2+} + P^{5+} + 3Al \rightarrow Co_2P + 3Al^{3+}$) designed (**Scheme 1** and **Figure S1**), which employs the phosphorus pentachloride (PCl_5) as the phosphorus source, cobalt dichloride ($CoCl_2$) as the cobalt source, aluminum trichloride and sodium chloride ($AlCl_3$-NaCl) as the low eutectic molten salt, and Al as the reducing agent. It is worth noting that the reaction process uses low-toxic PCl_5 as the phosphorus source, avoiding the release of highly poisonous PH_3 and flammable organic phosphorus sources, significantly improving safety. The crystal structures of the as-prepared sample were determined by powder X-ray diffraction (PXRD), as shown in **Figure 1a**. The sample matches well with Co_2P (JCPDS: 32-0306), indicating that they represent a unitary crystalline product. Scanning electron microscopy (SEM, **Figure 1b-1c**) and transmission electron microscopy (TEM, **Figure 1d**) shows that the as-prepared Co_2P presents uniform nanodendritic morphology. The lattice spacing in the high-resolution TEM (HRTEM) image was measured to be 2.21 or 2.23 Å (**Figure 1e**), corresponding to the (121) planes of Co_2P (JCPDS: 32-0306). The selected area electron diffraction (SAED) patterns are shown in **Figure 1f**. The several evident diffraction rings suggest the polycrystalline structure feature of as-prepared Co_2P. The result was consistent with PXRD analysis. **Figure 1g-1i** exhibits the scaling transmission electron microscopy energy dispersive spectroscopy (STEM-EDS) elemental mapping, and the results show a uniform distribution of Co and P in the as-prepared Co_2P nanodendrites.

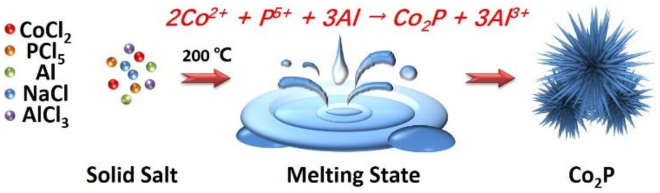

Scheme 1. Synthetic procedures of Co_2P nanodendrites.

The surface chemical composition of the Co_2P nanodendrites was further proved by X-ray photoelectron spectroscopy (XPS). In **Figure 2a**, the XPS survey spectra indicate the spectroscopic features of Co, P, O, and C. The high-resolution XPS spectrum of the Co presents of Co 2p, showing peaks at 792.8 eV and 778.0 eV, the characteristic peaks of Co-P corresponding to the Co $2p_{1/2}$ and Co $2p_{3/2}$, respectively, as shown in **Figure 2b**.[45] Meanwhile, there are two satellite peaks centered at 786.1, 802.5 eV and the peaks at 781.1 eV and 797.3 eV ascribed to Co-O bonding in oxidized Co species. Additionally, in the XPS spectrum of P 2p (**Figure 2c**), two peaks with binding energy of 130.3 and 129.2 eV arise from P $2p_{1/2}$ and P $2p_{3/2}$, respectively, which can be assigned to P-Co form in transition metal phosphides (TMPs) crystal, while the distinct peak at 133.0 eV be caused by the oxidized P species.[45] It should be noted that the slight surface oxidation is a widespread phenomenon for TMPs nanomaterials by virtue of contact with air, which is consistent with many studies published in the literature.[45, 46]

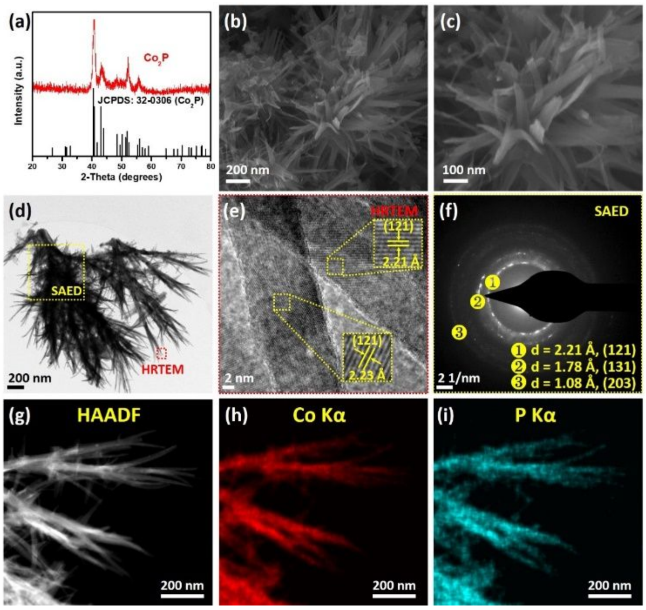

Figure 1. (a) PXRD pattern of molten-salts-assisted synthesis of Co_2P nanodendrites. (b, c) SEM images of Co_2P. (d) TEM image, (e) HRTEM image, and (f) SAED pattern, of Co_2P, respectively. (g) HAADF image and corresponding EDS elemental mapping images (h, i) of Co_2P.

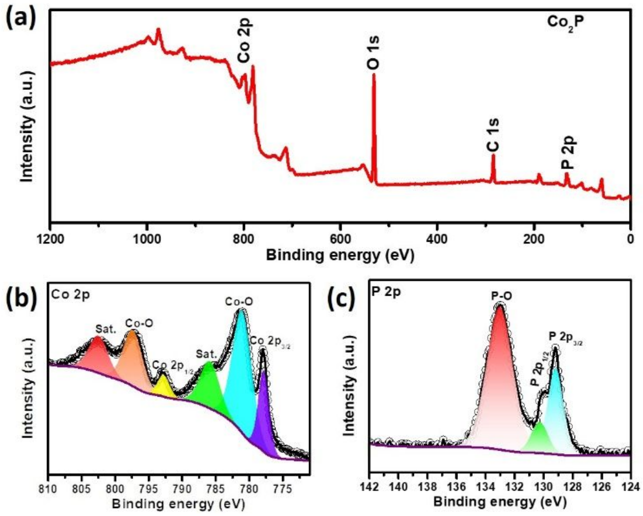

Figure 2. (a) XPS analysis of Co_2P. High-resolution XPS (b) Co 2p and (c) P 2p spectra of Co_2P.

The catalytic behavior of Co_2P nanodendrites and contrastive sample (carbon black) toward NO_3^-RR were evaluated in a typically three-electrode system in 0.5 M Na_2SO_4 with 0.1 M $NaNO_3$ (see **Supporting Information**). The linear sweep voltammetry (LSV) technique was applied to estimate the electrocatalytic activity of the samples. All the potentials in this work are regulated by a reversible hydrogen electrode (RHE). As shown in **Figure 3a**, the LSV polarization curves without iR-corrected shows that Co_2P nanodendrites manifests outstanding NO_3^-RR performance whereas carbon black possesses poor NO_3^-RR activity. Co_2P nanodendrites only requires applied potential of -0.24 V to achieve current density of 10 mA cm^{-2}, significantly positive than -0.86 V of carbon black. The selectivity of the Co_2P nanodendrites towards the NO_3^-RR was further investigated using chronoamperometry measurements at different applied potentials, as shown in **Figure 3b**. After 1 h running, ammonia, the reduction products of NO_3^-RR, was detected by ^{1}H nuclear magnetic resonance (^{1}H NMR, **Figure S2-S3**) spectra (other possible reductive products included NO_x, N_2, N_2H_4, and H_2, *etc.* were not detected), as shown in **Figure 3c**. The results show that NH_3 can be produced at -0.3 V, and the Faradaic efficiency (FE, **Table S2**) of NH_3 is 70.98% and close to ~90% at -0.4 V~-0.6 V. In **Figure 3d** and **Figure S4**, in order to eliminate the influence of environment, electrode, and nitrogen source, we conducted blank contrast experiment. The results showed that ammonia generation could not be detected in the absence of nitrate, indicating that the NH_3 in the above products was mainly from NO_3^-RR.

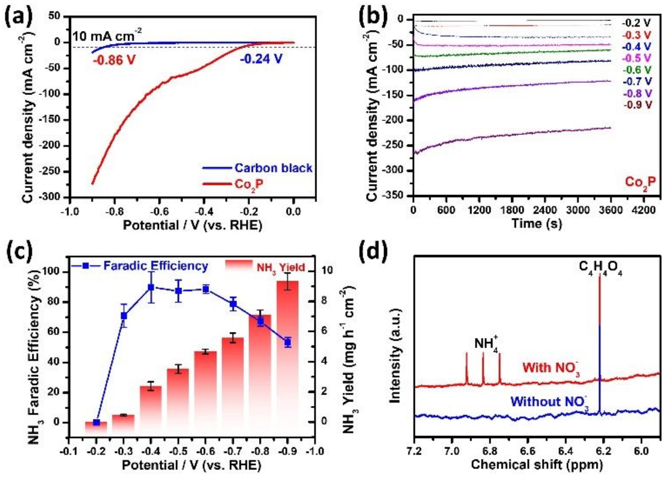

Figure 3. (a) NO_3^-RR polarization curves for Co_2P nanodendrites and carbon black in 0.5 M Na_2SO_4 with or without 0.1 M $NaNO_3$ solution. (b) The chronoamperometric response of Co_2P nanodendrites in 0.5 M Na_2SO_4 with 0.1 M $NaNO_3$ solution at different potentials. (c) NH_3 yields and FEs of Co_2P nanodendrites for the NO_3^-RR at different potentials. (d) The ^{1}H NMR spectra of catholyte in 0.5 M Na_2SO_4 with or without 0.1 M $NaNO_3$ solution at -0.8 V vs. RHE.

The electrocatalytic cycle stability is another vital performance metric to consider when selecting a catalyst for NO_3^-RR. Based on the consideration of NH_3 yield and FE, -0.6 V is the preferred potential of NO_3^-RR to evaluate the long-term stability of Co_2P nanodendrites. As shown in **Figure 4a**, in each electrolysis cycle, the current density of electrolysis gradually decreases with the electrolysis, which is caused by the constant consumption of NO_3^-. It is worth pointing out that the current recovers as usual after the electrolyte is refreshed, which can stabilize the cycle for 10 times, indicating that Co_2P nanodendrites has excellent NO_3^-RR catalytic stability. In addition, in 10 cycle tests, the average Faraday efficiency of Co_2P nanodendrites catalyzed NO_3^-RR reached 88.57%, and the average yield reached 5.11 mg cm^{-2} h^{-1}, as shown in **Figure 4b** and **Table S3**. Moreover, XRD (**Figure S5**) and SEM (**Figure S6**) results show that Co_2P nanodendrites still retains the original Co_2P (JCPDS: 32-0306) crystal structure and nanodendrite morphology after the stability test, further indicating that as-prepared Co_2P nanodendrites has good electrocatalytic stability.

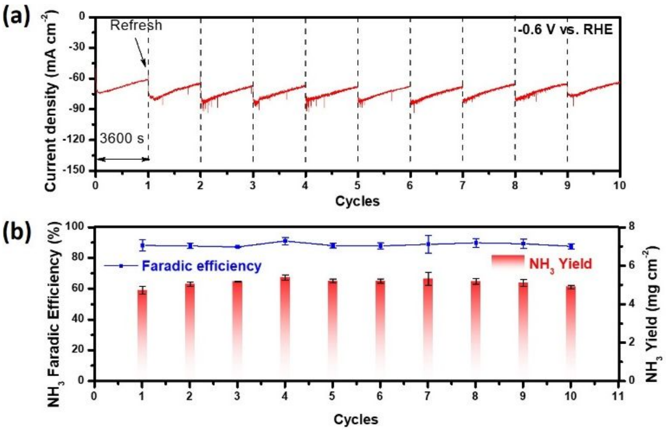

Figure 4. (a) The consecutive recycling test for Co_2P nanodendrites at –0.80 V and corresponding (b) NH_3 yields and FEs.

In summary, we designed a low toxicity and one-step molten salt synthesis method to synthesize Co_2P with nanodendritic morphology. The potential application of the as-prepared Co_2P nanodendrites in NO_3^-RR was discussed. At specific potential, the FE of the Co_2P nanodendrites electrocatalytic reduction of nitrate to ammonia can approach 90%, and it can be stably cycled for more than 10 times. Our research provides new insights into the synthesis of TMPs and the development of catalyst systems for ammonia production by nitrate reduction.

This work was financially supported by the National Natural Science Foundation of China (No. 22225902, U22A20436), the National key Research & Development Program of China (2022YFE0115900, 2021YFA1501500), the CAS-Commonwealth Scientific and Industrial Research Organization (CSIRO) Joint Research Projects (121835KYSB20200039), the Joint Fund of the Yulin University and the Dalian National Laboratory for Clean Energy (Grant. YLU-DNL Fund 2021011), Fujian Province Central Government Guides to Science and Technology Development Special Project (No. 2022L3024), and China Postdoctoral Science Foundation (No. 2021M703216).

Conflicts of interest

There are no conflicts to declare.

Author contributions

Luocai Yi: Conceptualization, Data curation, Funding acquisition, Investigation, Supervision, Writing – original draft, Writing – review & editing; **Ping Shao:** Data curation, Writing – review & editing. **Zhenhai Wen:** Conceptualization, Funding acquisition, Supervision, Validation, Writing – review & editing

Notes and references

1. J. Crawford, H. Yin, A. Du and A. P. O'Mullane, *Angew. Chem. Int. Ed.*, 2022, **134**, 202201604.
2. R. Daiyan, T. Tran-Phu, P. Kumar, K. Iputera, Z. Tong, J. Leverett, M. H. A. Khan, A. Asghar Esmailpour, A. Jalili, M. Lim, A. Tricoli, R.-S. Liu, X. Lu, E. Lovell and R. Amal, *Energy Environ. Sci.*, 2021, **14**, 3588-3598.
3. J. Qin, C. Pei, C. Zhao, Z. Lu, G. Sun and J. Gong, *ACS Sustain. Chem. Eng.*, 2022, **10**, 6999-7009.
4. J. Lim, C. A. Fernández, S. W. Lee and M. C. Hatzell, *ACS Energy Lett.*, 2021, **6**, 3676-3685.
5. R. Li, K. Xiang, Z. Liu, Z. Peng, Y. Zou and S. Wang, *Adv. Funct. Mater.*, 2022, **32**, 2208212.
6. H. Niu, Z. Zhang, X. Wang, X. Wan, C. Shao and Y. Guo, *Adv. Funct. Mater.*, 2021, **31**, 2008533.
7. Y. Cui, A. Dong, Y. Qu, J. Zhang, M. Zhao, Z. Wang and Q. Jiang, *Chem. Eng. J.*, 2021, **426**, 131843.
8. N. R. Singstock and C. B. Musgrave, *J. Am. Chem. Soc.*, 2022, **144**, 12800-12806.
9. Z. Dai, W. Wang, Z. Wang, S. Wang, H. Yu, Y. Xu, X. Li, L. Wang and H. Wang, *Chem. Commun.*, 2022, **58**, 6088-6091.
10. R. Jia, Y. Wang, C. Wang, Y. Ling, Y. Yu and B. Zhang, *ACS Catal.*, 2020, **10**, 3533-3540.
11. Y. Wang, A. Xu, Z. Wang, L. Huang, J. Li, F. Li, J. Wicks, M. Luo, D. H. Nam, C. S. Tan, Y. Ding, J. Wu, Y. Lum, C. T. Dinh, D. Sinton, G. Zheng and E. H. Sargent, *J. Am. Chem. Soc.*, 2020, **142**, 5702-5708.
12. Y. Xu, Y. Sheng, M. Wang, T. Ren, K. Shi, Z. Wang, X. Li, L. Wang and H. Wang, *J. Mater. Chem. A*, 2022, **10**, 16883-16890.
13. Z. Tao, Y. Wu, Z. Wu, B. Shang, C. Rooney and H. Wang, *J. Energy Chem.*, 2022, **65**, 367-370.
14. Q. Hu, Y. Qin, X. Wang, H. Zheng, K. Gao, H. Yang, P. Zhang, M. Shao and C. He, *CCS Chemistry*, 2022, **4**, 2053-2064.
15. G.-F. Chen, Y. Yuan, H. Jiang, S.-Y. Ren, L.-X. Ding, L. Ma, T. Wu, J. Lu and H. Wang, *Nature Energy*, 2020, **5**, 605-613.
16. J. M. McEnaney, S. J. Blair, A. C. Nielander, J. A. Schwalbe, D. M. Koshy, M. Cargnello and T. F. Jaramillo, *ACS Sustain. Chem. Eng.*, 2020, **8**, 2672-2681.
17. M. S. El-Deab, *Electrochim. Acta*, 2004, **49**, 1639-1645.
18. H. Liu, J. Park, Y. Chen, Y. Qiu, Y. Cheng, K. Srivastava, S. Gu, B. H. Shanks, L. T. Roling and W. Li, *ACS Catal.*, 2021, **11**, 8431-8442.
19. S. Taguchi and J. M. Feliu, *Electrochim. Acta*, 2007, **52**, 6023-6033.
20. J. Li, G. Zhan, J. Yang, F. Quan, C. Mao, Y. Liu, B. Wang, F. Lei, L. Li, A. W. M. Chan, L. Xu, Y. Shi, Y. Du, W. Hao, P. K. Wong, J. Wang, S. X. Dou, L. Zhang and J. C. Yu, *J. Am. Chem. Soc.*, 2020, **142**, 7036-7046.
21. Y. Guo, X. Cai, S. Shen, G. Wang and J. Zhang, *J. Catal.*, 2021, **402**, 1-9.
22. Y. Han, X. Zhang, W. Cai, H. Zhao, Y. Zhang, Y. Sun, Z. Hu, S. Li, J. Lai and L. Wang, *J. Colloid Interf. Sci.*, 2021, **600**, 620-628.
23. X. Zhang, C. Wang, Y. Guo, B. Zhang, Y. Wang and Y. Yu, *J. Mater. Chem. A*, 2022, **10**, 6448-6453.
24. F. Y. Chen, Z. Y. Wu, S. Gupta, D. J. Rivera, S. V. Lambeets, S. Pecaut, J. Y. T. Kim, P. Zhu, Y. Z. Finfrock, D. M. Meira, G. King, G. Gao, W. Xu, D. A. Cullen, H. Zhou, Y. Han, D. E. Perea, C. L. Muhich and H. Wang, *Nat. Nanotechnol.*, 2022, **17**, 759-767.
25. J. Liang, Q. Liu, A. A. Alshehri and X. Sun, *Nano Res. Energy*, 2022, **1**, e9120010.
26. Q. Chen, J. Liang, L. Yue, Y. Luo, Q. Liu, N. Li, A. A. Alshehri, T. Li, H. Guo and X. Sun, *Chem. Commun.*, 2022, **58**, 5901-5904.
27. X. Deng, Y. Yang, L. Wang, X. Z. Fu and J. L. Luo, *Adv. Sci.*, 2021, **8**, 2004523.
28. X. Xu, L. Hu, Z. Li, L. Xie, S. Sun, L. Zhang, J. Li, Y. Luo, X. Yan, M. S. Hamdy, Q. Kong, X. Sun and Q. Liu, *Sustain. Energ. Fuels*, 2022, **6**, 4130-4136.
29. Z. Li, J. Liang, Q. Liu, L. Xie, L. Zhang, Y. Ren, L. Yue, N. Li, B. Tang, A. A. Alshehri, M. S. Hamdy, Y. Luo, Q. Kong and X. Sun, *Mater. Today Phys.*, 2022, **23**, 100619.
30. Z. Deng, C. Ma, Z. Li, Y. Luo, L. Zhang, S. Sun, Q. Liu, J. Du, Q. Lu, B. Zheng and X. Sun, *ACS Appl. Mater. Interfaces*, 2022, **14**, 46595-46602.
31. Z. Deng, C. Ma, X. Fan, Z. Li, Y. Luo, S. Sun, D. Zheng, Q. Liu, J. Du, Q. Lu, B. Zheng and X. Sun, *Mater. Today Phys.*, 2022, **28**, 100854.
32. W.-D. Zhang, H. Dong, L. Zhou, H. Xu, H.-R. Wang, X. Yan, Y. Jiang, J. Zhang and Z.-G. Gu, *Appl. Catal. B-Environ.*, 2022, **317**, 121750.
33. Q. Song, M. Li, X. Hou, J. Li, Z. Dong, S. Zhang, L. Yang and X. Liu, *Appl. Catal. B-Environ.*, 2022, **317**, 121721.
34. X. Zhang, G. Ma, L. Shui, G. Zhou and X. Wang, *Chem. Eng. J.*, 2022, **430**, 132666.
35. R. Zhang, Y. Guo, S. Zhang, D. Chen, Y. Zhao, Z. Huang, L. Ma, P. Li, Q. Yang, G. Liang and C. Zhi, *Adv. Energy Mater.*, 2022, **12**, 2103872.
36. A. Iarchuk, A. Dutta and P. Broekmann, *J. Hazard. Mater.*, 2022, **439**, 129504.
37. Q. Liu, L. Xie, J. Liang, Y. Ren, Y. Wang, L. Zhang, L. Yue, T. Li, Y. Luo, N. Li, B. Tang, Y. Liu, S. Gao, A. A. Alshehri, I. Shakir, P. O. Agboola, Q. Kong, Q. Wang, D. Ma and X. Sun, *Small*, 2022, **18**, 2106961.
38. J. Li, M. Li, N. An, S. Zhang, Q. Song, Y. Yang, J. Li and X. Liu, *Proc. Natl. Acad. Sci. USA*, 2022, **119**, e2123450119.
39. J.-X. Liu, D. Richards, N. Singh and B. R. Goldsmith, *ACS Catal.*, 2019, **9**, 7052-7064.
40. S. Ye, Z. Chen, G. Zhang, W. Chen, C. Peng, X. Yang, L. Zheng, Y. Li, X. Ren, H. Cao, D. Xue, J. Qiu, Q. Zhang and J. Liu, *Energy Environ. Sci.*, 2022, **15**, 760-770.
41. Y. Jia, Y. G. Ji, Q. Xue, F. M. Li, G. T. Zhao, P. J. Jin, S. N. Li and Y. Chen, *ACS Appl. Mater. Interf.*, 2021, **13**, 45521-45527.
42. J. Wang, C. Cai, Y. Wang, X. Yang, D. Wu, Y. Zhu, M. Li, M. Gu and M. Shao, *ACS Catal.*, 2021, **11**, 15135-15140.
43. H. B. Huang, S. H. Luo, C. L. Liu, T. F. Yi, Y. C. Zhai, *ACS Appl. Mater. Interf.*, 2018, **10**, 21281-21290.
44. Y. Shi, M. Li, Y. Yu and B. Zhang, *Energy Environ. Sci.*, 2020, **13**, 4564-4582.
45. S. Yang, G. Chen, A. G. Ricciardulli, P. Zhang, Z. Zhang, H. Shi, J. Ma, J. Zhang, P. W. M. Blom and X. Feng, *Angew. Chem. Int. Ed.*, 2020, **59**, 465-470.
46. Y. Hou, Y. Liu, R. Gao, Q. Li, H. Guo, A. Goswami, R. Zboril, M. B. Gawande and X. Zou, *ACS Catal.*, 2017, **7**, 7038-7042.